Physisorption and Chemisorption of Some *n*-Hydrocarbons at the Brønsted Acid Site in Zeolites 12-Membered Ring Main Channels: Ab Initio Study of the Gmelinite Structure

L. Benco[†,‡,*] J. Hafner,[†] F. Hutschka,[§] and H. Toulhoat[||]

Institut für Materialphysik and Center for Computational Materials Science, Universität Wien, Sensengasse 8, A-1090 Wien, Austria, Institute of Inorganic Chemistry, Slovak Academy of Sciences, Dubravska cesta 9, SK-84236 Bratislava, Slovak Republic, Totalfinaelf, Centre Européen de Recherche et Technique, B. P. 27, F-76700 Harfleur, France, and Institut Français du Pétrole, F-92852 Rueil-Malmaison Cedex, France

Received: December 5, 2002; In Final Form: June 3, 2003

An ab initio density-functional investigation of the physisorption and chemisorption of neutral and protonated *n*-olefins in the zeolitic 12-membered ring main channel of a zeolite has been performed for gmelinite. A linear increase of the energy of physisorption with the length of the hydrocarbon is observed in agreement with experimental data. Upon chemisorption, a covalent C(olefin)-to-O(zeolite) bond is formed producing a stable alkoxy species. The energy of chemisorption depends on both the zeolite O-site and the length of the olefin chain. Shorter molecules (ethene and propene) chemisorbed at any of the crystallographically inequivalent O-sites on the inner surface of the zeolite (O1, O3, and O4) are more stable than physisorbed species. With the increasing length of the molecule the chemisorption energy decreases due to the deformation necessary to accommodate the molecule within the channel and due to the increasing repulsion between the molecule and the zeolite. The smallest deformation and repulsion is observed for the O4-site where chemisorbed molecules of any length are more stable than the physisorbed species. Better stabilization at the O4-site is achieved because of a more symmetric contact allowing the formation of the shortest and most stabilizing C−O bond. The chemisorption at the zeolite inner surface thus represents a possible reaction channel for the conversion of olefins in zeolites. Protonated molecules of short olefins (ethene, propene) collapse to neutral hydrocarbons. The cations formed by the protonation of butene and pentene are relatively stable in the zeolite disfavored by only ∼+70 kJ/mol as compared with chemisorbed species. Longer protonated molecules show increased stability with increasing chain length.

1. Introduction

Zeolites are microporous aluminosilicates with many applications as acid catalysts, widely used in petroleum and chemical industries for a number of commercially important hydrocarbon reactions.[1,2] The complete mechanism of hydrocarbon (HC) conversion is rather complex, comprising several partial reconstructions such as C−C bond breaking, C−C bond-forming, alkyl group shift (isomerization), single or multiple proton transfer, de- and rehydrogenation, etc. Not surprisingly, the detailed mechanism of intrazeolite conversions is still not completely clear.

The contact of the HC with the H-zeolite can cause either protonation of the neutral molecule or the extraction of an hydride anion.[3,4] Two kinds of ions can be produced this way. A carbenium cation forms upon protonation of an olefin or upon hydride extraction from a paraffin. Except classical cation, where the positive charge is localized at the three-coordinated carbon atom, a formation of nonclassical carbocation also occurs with delocalized (bridged) bonding of π- or σ-electrons.[5] Second kind is carbonium cation that forms via protonation of paraffins. Due to the overcoordination of one carbon atom carbonium cation collapses to give carbenium ions, as in Olah's superacid chemistry.[6]

Without any direct evidence, carbenium and carbonium ions were for a long time accepted as intermediate species stabilized in the polar zeolite surroundings by long-range electrostatic interactions. Recent solid-state NMR and IR experiments show, however, that adsorbed protonated HC molecules are not stable. Instead, covalent bonds between zeolite O-atoms and C atoms are observed.[7−9] Subsequently, new experimental findings corroborated by theoretical studies confirm the increased stability of surface alkoxy species compared with adsorbed protonated HC molecules.[10−12] The discovery of alkoxy species as intermediates of the HC conversion initiated the development of novel scenarios for various intrazeolite reactions. Furtado et al. report activation energies for the chemisorption of ethane, propane, and isobutane in the zeolite.[13] They assume that formation of a covalent bond between the saturated molecule and the zeolite framework is enabled by the attack of the Brønsted acid proton on the molecule accompanied by the liberation of the dihydrogen molecule. Isomerization of toluene, xylene, and dimethyldibenzothiophene over mordenite with alkoxy species as reaction intermediate has been investigated by Rozanska et al.[14] Demuth et al.[15] report isomerization of pentene over H-ZSM-22 with dimethylcyclopropane as a reaction intermediate. Cracking of small paraffins in zeolites also leads to the formation of alkoxy intermediates. Reaction barriers resulting from an extended cluster model[16] compare reasonably well with those from the periodical approach.[17] The

* To whom correspondence should be addressed. Tel: +43-1-4277-51407. Fax: +43-1-4277-9413. E-mail: lubomir.benco@univie.ac.at.
† Universität Wien.
‡ Slovak Academy of Sciences.
§ Totalfinaelf.
|| Institut Français du Pétrole.

10.1021/jp027625z CCC: $25.00
Published on Web 08/12/2003

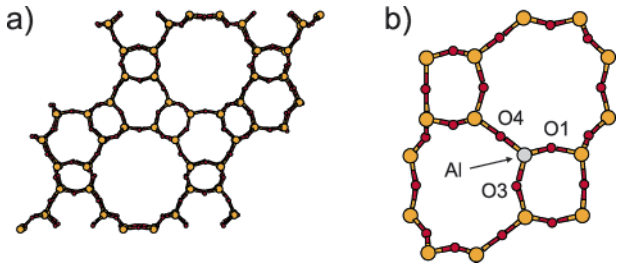

Figure 1. Structural model. Hexagonal framework of gmelinite looking down the *c*-axis (a). Fragment of the zeolite framework in the main channel showing the location of the Al-site and of the O1-, O3-, and O4-sites (b). The O2-site is not accessible from the main channel.

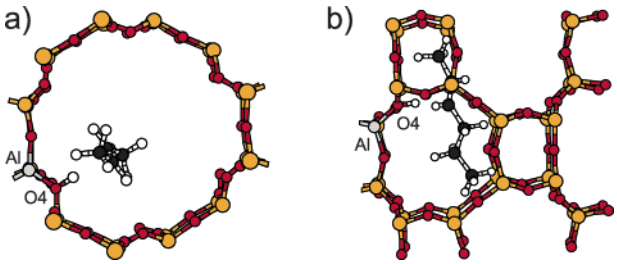

Figure 2. Physisorbed molecule in gmelinite. Top view (a) and the side view (b) of the location of the adsorbed molecule in the main channel of zeolite. The acid H atom resides at the O4 atom pointing to the double bond of the olefin.

influence of the local zeolite geometry on the stability of alkoxide intermediates is investigated by Boronat et al.[18] They find that chemisorbed species are very sensitive to the local geometry of the active site of their model zeolite cluster.

In the present work we report DFT simulations of the chemisorption of olefins in zeolite. We use a periodic approach—this eliminates drawbacks of the cluster modeling, such as cluster size effect, large artificial surface, neglect of long-range electrostatic interactions, etc. Simulations are performed for gmelinite. This particular zeolite is interesting because it is composed of same secondary building units (hexagonal prisms) as faujasites—a widely used materials in industrial catalysis. The smaller unit cell of gmelinite, however, makes these calculations computationally affordable. Due to a relatively high symmetry, only four O-sites are crystallographically inequivalent. The small number of irreducible O-sites of the zeolite enables the comparison of the chemisorption at all positions of the zeolite situated in the main channel. The cavity of the zeolite, however, is large enough to accommodate HC molecules up to straight *n*-hexene, or deformed *n*-heptene. We compare the bonding of a series of unsaturated *n*-hydrocarbons from ethene to hexene (or heptene). Moreover, the energetics of the chemisorbed species is compared with that of the physisorbed molecules and with the energetics and stabilities of corresponding carbenium cations.

2. Structural Model

Gmelinite is good candidate for ab initio simulations of intrazeolite phenomena. The structure contains both large cavities and relatively small connecting channels (Figure 1a).[19] The gmelinite cage and the hexagonal prism are also constituting elements of the crystal structure of faujasites, which are industrially important zeolites. The kinetic diameter of the main channel of ~7 Å is comparable with those of large pore zeolites.[20] Purely siliceous gmelinite has the composition $Si_{24}O_{48}$ and forms a hexagonal structure with space group $P6_3mmc$. The cell dimensions are $a = b = 13.756$ Å and $c = 10.048$ Å.[19] The stacking of the building blocks leads to a columnar structure with prisms and gmelinite cages alternating along each column. The largest cavity is circumscribed by a ring of twelve SiO_4 tetrahedra (the twelve-membered ring—12MR, cf. Figure 1a) parallel with the *c*-axis. Due to the high space-group symmetry all tetrahedral sites (Si/Al) are crystallographically equivalent and there are only four inequivalent O sites. Three of the O-sites are located at the inner surface of the main cavity (O1, O3, and O4, cf. Figure 1b) and the O2-site is accessible only from the gmelinite cage. The rather uniform shape of the unit cell allows the insertion of relatively long particles, such as *n*-hexane (Figures 2a and 2b) or a deformed *n*-heptane. Figure 3, parts a and b, display an example of such a deformed heptane molecule chemisorbed within the main channel of gmelinite.

Simulations are performed with the experimental unit cell determined on hydrated Na-form of gmelinite.[19] As pointed out in our previous work,[21] no significant change of the cell shape is observed with the relaxation of the shape of the zeolite. A dehydration of the zeolite always causes a shrinking of the unit cell. Our computational technique based on DFT and GGA (cf. below), however, provides slightly expanded unit cells. Thus, the experimental unit cell volume compares well with that resulting from the optimization procedure.[21] In this work, only adsorption at the Brønsted acid sites is considered. The acid site is produced by one Al/Si substitution (Si/Al = 23). The neglect of extraframework cations and their influence on the geometry of the zeolite framework is compensated by full relaxation of all atomic positions.

3. Calculational Details

Ab initio periodic total-energy calculations are performed to describe the fully relaxed crystal structure. The calculations are based on density-functional theory[22] using the generalized-gradient approximation (GGA) to the exchange-correlation functional as developed by Perdew and Wang (PW91).[23,24] We use ultrasoft pseudopotentials[25,26] and a plane-wave basis as implemented in the Vienna ab initio simulation package VASP.[27] The calculations are performed using Blöchl's projector augmented wave technique[28,29] with a plane-wave cutoff energy of 400 eV. Due to the large volume of the unit cell Brillouin-zone sampling is restricted to the Γ-point. Convergence is improved using a modest smearing of the eigenvalues. The optimization of atomic geometries is performed via a conjugate-gradient algorithm with the break condition for the electronic self-consistency loop of 10^{-5} eV for the total energy of the cell. In the relaxation procedure, no symmetry restrictions are applied.

4. Results

4.1 Adsorption Energies. Adsorption energies of olefins are calculated as the difference between the total energy of the complex *E*(zeo + HC) and the sum of the energies of the separated fragments

$$E_{ads} = E(\text{zeo} + \text{HC}) - E(\text{zeo}) - E(\text{HC}) \qquad (1)$$

where *E*(zeo) is the energy of the adsorbate-free H-form of the zeolite, and *E*(HC) is energy of the hydrocarbon molecule in vacuo. Calculated energies for both physisorption and chemisorption of olefins are displayed in Figure 4. For sake of comparison, Figure 4 displays also the calculated adsorption energies of paraffins reported in our previous work.[30]

Physisorption. To simulate physisorption at the acid site of the zeolite the linear olefins C2—C6 are inserted in the gmelinite main channel and extended along the channel (cf. Figure 2a and 2b). The double bond is placed close to the zeolite acid

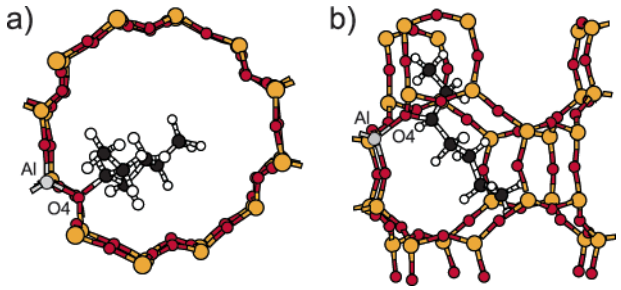

Figure 3. Chemisorbed molecule in gmelinite. Top view (a) and side view (b) of the main channel with olefin chemisorbed at the O4 site.

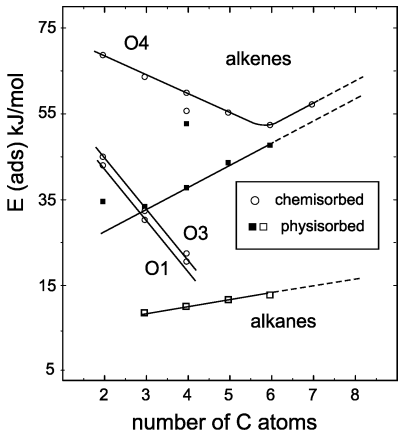

Figure 4. Energies of physisorption and chemisorption of *n*-alkanes and *n*-alkenes in the zeolite main channel. Alkenes are chemisorbed at O1-, O3-, and O4-sites. Full and dashed lines are guide to the eye.

site in order to enable an effective contact between the π-electron density and the Brønsted acid hydrogen atom. The adsorption energy of physisorbed molecules increases linearly with the chain length of the adsorbed alkene with an increment of ~5 kJ/mol per additional CH_2 group. No experimental data on gmelinite are available for comparison.

A linear character of the increase of the calculated adsorption energy with the length of the molecular chain is observed for both olefins and paraffins (cf. Figure 4) and compares favorably with the increase of the heats of adsorption measured for hydrocarbons in different zeolite structures, such as silicalite,[31] BEA, TON, MOR, FAU,[32] and TON, FER, and KFI[33] types of zeolites. For paraffins adsorbed in the acid zeolite, the calculated energies are too small. The neglect of dispersion forces in DFT (GGA) leads to values typically ~2.5 times smaller than experimental data. For propane, e.g., the calculated value is ~12 kJ/mol[30] and the estimated experimental value is ~30−36 kJ/mol.

For olefins the calculated adsorption energies are much higher than those of paraffins (cf. Figure 4). The value obtained for propene (33.4 kJ/mol) is comparable with the estimated adsorption energy of propane of ~30−36 kJ/mol. Our calculated energies reasonably compare with results by Boronat et al.[18] who use the same PW91 functional. For physisorption of *n*-butene at clusters of various size they report the value of ~27 kJ/mol and the complementary periodical calculation provides a value of ~38 kJ/mol. Our calculated adsorption energy at the inner surface of gmelinite is 37.8 kJ/mol (Figure 4). The computational DFT (GGA) procedure thus seem to provide realistic adsorption energies for olefins, which develop much stronger interactions with the acid solid than paraffins.

The adsorption energy of hydrocarbons adsorbed in zeolites consists of two components. The first is the interaction energy derived from the stabilizing overlap of the electron densities of of interacting atoms. This kind of interaction is either of covalent or of hydrogen-bonded character and exhibits rather strong directional properties. The use of the GGA functionals of the density-functional theory leads to satisfactory description of both covalent and hydrogen bonding. The second component of the adsorption energy is the dispersion energy. Weak interactions behind dispersion forces, however, are difficult to treat. Both generations of functionals, LDA and GGA, fail to describe weak interactions properly. In the LDA the bond-strength is considerably overvalued. By coincidence this can lead in those cases where dispersion forces are important to adsorption energies in numerical agreement with experiment, but the bonding mechanism is not correctly described. Although the GGA approach performs much better for strong interactions, dispersion forces (which depend on dynamical polarizabilities of the interacting species) are not properly described.

The measured heats of adsorption of saturated and unsaturated molecules of the same length in acid zeolites exhibit similar values.[34,35] Though calculated adsorption energy of olefins are comparable with experimental data, those of paraffins are ~2.5 times smaller.[30] Let us suppose that the adsorption energy of both propane and propene equals to ~35 kJ/mol. Then for propane the DFT (GGA) approach, providing ~12 kJ/mol,[30] comprises only 34%. Recently, Eder and Lercher have measured the contribution of the acid site to the heat of adsorption of saturated hydrocarbons in zeolites.[36] They report that the interaction energy is independent of the hydrocarbon chain and equals to ~7 kJ/mol and ~10 kJ/mol for MFI and FAU zeolites, respectively. For gmelinite with the framework density between those of MFI and FAU (~14.5 tetrahedral atoms/nm^3) and closer to FAU, we estimate the energy of interaction with the acid site at ~9 kJ/mol. The calculated adsorption energy of ~12 kJ/mol is thus composed of the interaction energy (~9 kJ/mol) and a contribution from dispersion interactions (~3 kJ/mol). Missing 66% could be attributed to the fraction of the dispersion energy neglected in the DFT calculation and to interactions with another types of active centers (Lewis sites) not considered in our calculation.

Although paraffins and olefins adsorbed in zeolites exhibit similar values of the adsorption energy,[34,35] considerably different components contribute to the latter. In a paraffin, only a small fraction of the energy comes from the bond-formation between the acid site and the adsorbed molecule. The majority is represented by the dispersion energy collected over a large number of small dynamical multipoles. Because the DFT does not account for the interaction between the induced dynamical multipoles the calculated adsorption energies are more than two times smaller than the measured heats of adsorption. The presence of the double bond in olefins leads to a weak covalent interaction between the acid site and the π-electron density of the molecule. The decrease of the distance between the sorbate and zeolite suppresses dispersive interactions, thus the dispersion energy represents only a small fraction of the adsorption energy. The adsorption energies of olefins calculated using DFT are therefore in reasonable agreement with experimental data.

Chemisorption. Chemisorbed molecules are extended along the main channel and connected via the covalent C−O bond to the zeolite O1-, O3-, and O4-site (cf. Figure 3a and 3b). Figure 4 shows that with increasing length of the hydrocarbon molecule the energy of chemisorption decreases for all O-sites. The zeolite O-sites, however, are clearly distinguished in two categories. For the O1- and O3-site the calculated reaction energies are similar and much smaller than for the O4-site. The adsorption energies of the ethylene molecule for O1-/O3- and O4-sites are

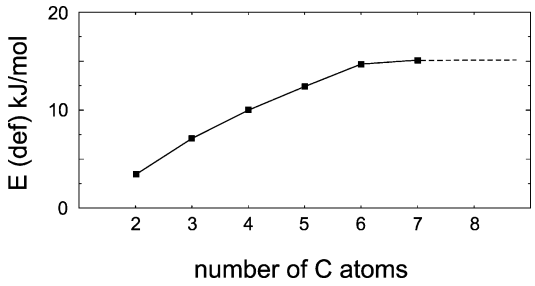

Figure 5. Energies of deformation of the linear olefin molecule relative to the ideal linear geometry.

~45 and ~70 kJ/mol, respectively. The decrease of the reaction energy for O1-/O3-sites is steeper (~13 kJ/mol per CH_2) than for the O4-site (~5 kJ/mol per CH_2). Moreover, for the C6 molecule at the O4-site the decrease of the calculated adsorption energy is smaller than indicated by the linear trend and for the C7 molecule the reaction energy increases to the value of ~57 kJ/mol higher than that of the C5 molecule (~55 kJ/mol).

Why does the physisorption energy increase with the length of the chain and energy of chemisorption decrease? The same trends are observed in the cluster calculations of Boronat et al.[18] They obtained negative values for the whole series of C2 to C4 molecules using the smallest cluster containing only three tetrahedral atoms. On larger clusters, the reaction energies are negative only for ethane and become positive already for C3 molecules. They concluded that with larger molecules due to the restrictions in the active site geometry the C-to-O distance increases, the covalent bond weakens and the alkoxy is energetically destabilized.

In the series of C2 to C7 alkoxy species chemisorbed at the O4-site of gmelinite we observe two phenomena causing a decrease of the chemisorption energy: A change of the local bonding and a deformation of the molecule. A detailed analysis of geometries around the molecule-to-zeolite contact are given in the paragraph below. There are two reasons for the deformation of the molecule: The local change of the geometry induced by the C−O bonding and a reorientation of the ends of the chemisorbed molecule leading to a reduction of the repulsion between adsorbate and substrate and allowing for the accommodation along the main channel of the periodical structure. Any deviation from the ideal linear geometry makes the particular configuration energetically disfavored and contributes to the decrease of the adsorption energy (Figure 4). To estimate the deformation energy, the total energies of the deformed molecules are calculated in vacuo and compared with the energies of fully relaxed structures. The geometries of the molecules are identical to those obtained from the relaxation of the alkoxy species bound to the O4-site of the zeolite. The former C−O bond is replaced by C−H bond of appropriate length. The calculated deformation energies are displayed in Figure 5. The ethene molecule with the geometry of the ethoxy complex is only by 3.4 kJ/mol less favorable than fully relaxed molecule. The deformation energy increases with the length of the molecule. The increase, however, is not linear and apparently saturates for molecules longer than C6. From C6 to C7 only a negligible increase of the deformation energy is observed (0.4 kJ/mol). The saturation is due to the elongation of the free end of the molecule that is placed at considerable distance from the zeolite and is not in the direct contact with the zeolite surface. Such an extension keeps linear shape of the molecule and therefore causes only slight increase of the deformation energy.

Note that the leveling off of the deformation energy upon extension from C6 to C7 corresponds with minimum in the adsorption energy (cf. Figure 4). This means that the decrease of the chemisorption energy is caused by the local deformation of the molecule in the neighborhood of the contact. The covalent C−O bond is as short as ~1.5 Å (cf. below). Via chemisorption the molecule is held at relatively short distance from the zeolite. Any unconstrained contact between a C−H fragment of the molecule and the O atoms of the zeolite network leads to the formation of a weak hydrogen bond with a bond-length larger than ~2.2 Å.[30] Because the covalent C−O bond keeps the molecule at much smaller distance, repulsion interactions prevail and the molecule deforms. The free ends of the molecule tend to move away from the inner surface of the zeolite into the channel, thus diminishing the repulsion between the molecule and the zeolite.

4.2 Geometries of Adsorbed Species. *Physisorption.* Because of the repulsion between the guest molecule and the host framework the largest adsorption energies are observed for molecules located in the largest channel of the zeolite. The adsorption in the gmelinite cage is disfavored by ~30 kJ/mol compared with the location in the main channel. The extended conformation along the channel is favored for these linear molecules. Upon physisorption of both paraffins and olefins the hydrocarbon molecule makes direct contact with the Brønsted acid site in the main channel. The molecule, however, remains located at a relatively large distance from the zeolite. For paraffin, the distance between the acid proton and the carbon atom of the adsorbed molecule is ~3.1 Å and the shortest contacts to H atoms of the molecule are as long as ~2.1 Å.[30] Planar arrangement of the double bond in olefins allows tighter contacts compared with paraffins. Distances of the acid proton to the C atoms of the double bond of the linear olefin are ~2.2 Å. Similar distances are found for benzene adsorbed in mordenite.[37] No pronounced changes of geometries of adsorbed molecules are observed compared with the ideal linear geometry. Similarly, no major changes of the local geometry occur around the zeolite acid site.

Chemisorption. Selected geometry parameters of ethene, propene, and butene chemisorbed at a O-site of the zeolite are given in Table 1. For the O4-site the series of chemisorbed hydrocarbons is extended up to the heptene molecule. The geometry of the chemisorption site and the labeling of atoms is displayed in Figure 6. Local changes of bonding, induced by the molecule-to-zeolite bond, are observed on both the molecular chain and the zeolite framework. The C−O bond established between the molecule and the zeolite is of covalent character. For all alkoxy species the bond-length is larger (~1.510 to ~1.590 Å) than the C−O distance in the alkylhydroxide (~1.485 Å). The distance is shortest for an ethoxy species. A monotonic increase with increasing hydrocarbon length is observed for all O-sites. This means that the increase of the length of the molecule increases the repulsion between the molecule and the zeolite. Consequently, the C−O distance increases and the stability of the chemisorbed cluster decreases. For a given molecule the C−O distances at the O1- and O3-site are similar and longer than at the O4-site. For the ethene molecule e.g., the corresponding distances are 1.530, 1.530, and 1.514 Å, respectively. The shorter C−O bond length indicates the higher stability of alkoxy species adsorbed at the O4-site. An exception from the monotonic increase is observed only for the heptene molecule adsorbed at the O4-site. The slight decrease from 1.572 Å for hexene to 1.570 Å for heptene indicates higher stability. This corresponds to the calculated energies of adsorption exhibiting an increased energy of chemisorption of heptene compared with hexene (Figure 4).

TABLE 1: Selected Geometry Parameters of Ethene (C2), Propene (C3) and Butene (C4) Molecules Chemisorbed to the O-sites of the Inner Surface of Gmelinite (distances in Å and angles in deg)[a]

O1-site	H-zeolite	C2	C3	C4
O(III)[b]−X[c]	0.978	1.530	1.577	1.588
Al−O(III)	1.908	1.921	1.931	1.936
Si−O(III)	1.710	1.706	1.703	1.705
Al−O(III)−Si	138	133	132	130
Al−O(III)−X	108	108	105	106
O(III)−C_2−C_1		111	108	111

O3-site	H-zeolite	C2	C3	C4
O(III)−X	0.976	1.530	1.575	1.587
Al−O(III)	1.915	1.923	1.925	1.926
Si−O(III)	1.719	1.718	1.715	1.713
Al−O(III)−Si	136	125	124	123
Al−O(III)−X	111	120	122	121
O(III)−C_2−C_1		115	111	110

O4-site	H-zeolite	C2	C3	C4	C5	C6	C7
O(III)−X	0.976	1.514	1.556	1.561	1.566	1.572	1.570
Al−O(III)	1.901	1.895	1.897	1.897	1.896	1.899	1.897
Si−O(III)	1.710	1.702	1.699	1.699	1.698	1.697	1.696
Al−O(III)−Si	136	131	129	129	130	129	129
Al−O(III)−X	111	110	109	109	109	109	108
O(III)−C_2−C_1		113	112	111	111	112	112

For the O4-site the Series of Hydrocarbons Is Extended up to Heptene (C7). [a] Chemisorption through the secondary carbon atom (cf. Figure 6). [b] O(III) denotes three-coordinated oxygen atom. [c] X stands for H in H-zeolite and for C in chemisorbed alkoxy species.

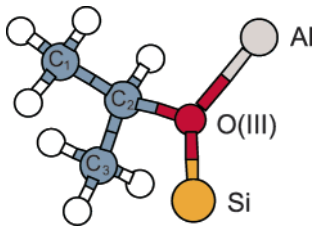

Figure 6. Geometry of the chemisorption site. A fragment of the inner zeolite surface is represented by the Al, O, and Si atoms, respectively. The molecule is chemisorbed to O via the secondary C atom.

Local changes of the framework bonding lead to a modification of Al−O and Si−O bonds and of the Al−O−Si angle. The Si−O bond undergoes the least variation. Upon chemisorption the Si−O bond-distance shortens compared with the H-form of the zeolite, E.g. chemisorption of butene at the O1- or O3-site leads to a shortening by ∼0.005 Å and a reduction by ∼0.010 Å is observed for the O4-site. More dramatic changes occur for the Al−O bond-length. Chemisorption of butene causes an elongation by 0.028 Å at the O1-site and by 0.011 Å at the O3-site. The O4-site, however, shows a different behavior. Upon chemisorption the Al−O distance shrinks to ∼1.897 Å and only a slight variation of the bond-length is observed with increasing length of the hydrocarbon. The Al−O−Si angles of the H-form of the zeolite show similar values for any of the O-sites (∼136°). Upon alkylation of any of the O-sites the formation of the third bond leads to the bonding of a bond of sp^2 character and the Al−O−Si angles decrease toward 120°.

A possible change of the orientation of the molecule relative to the zeolite framework is reflected by changes of Al−O−X and O−C−C angles (cf. Figure 6). The comparison of Al−O−H and Al−O−C angles shows that at the O1- and O4-sites the local geometry of the H-form and of the alkoxy species is similar. Alkylation at the O3-site, however, leads to a change of the angle from ∼110° to ∼120°. Only a small variation of the O−C_2−C_1 angle occurs. For longer molecules, a slight decrease is observed. A larger angle means that the molecule rotates away from the zeolite, thus decreasing the repulsion between the molecule and the zeolite framework. The parameters collected in Table 1 show that only small molecules can behave this way. For longer molecules accommodated in the zeolite channel, the O−C−C angle remains smaller, indicating larger destabilizing repulsion compared with shorter molecules.

TABLE 2: Selected Geometry Parameters of Propene Chemisorbed at Different O-sites (distances in Å and angles in deg)[a]

	O1-site	O3-site	O4-site
O(III)−C_2	1.577	1.575	1.556
C_1−C_2	1.514	1.507	1.511
C_2−C_3	1.508	1.515	1.511
H···O[b]	2.23	2.38	2.27
	2.46	2.44	2.46
	2.53	2.75	2.67
C_1−C_2−C_3	117	112	116

[a] Notation as in Table 1. [b] Shortest H-to-O contacts between the molecule and the framework.

Selected parameters of propene chemisorbed at different O-sites to form an isopropoxy species (Figure 6) are given in Table 2. Upon adsorption at the O1- and O3-site an asymmetry in the C−C bonding occurs. For both sites a shortening of one C−C bond and elongation of the other one is observed. The molecule connected to the O4-site is relaxed to a symmetrical shape with C−C bonds of equal length. The C−C−C angles of the O1- and O4-sites are of similar value (∼116°). For the O3-site the C−C−C angle is decreased. An important factor driving the stability of the alkoxy species could in principle be H···O contacts between the molecule and the zeolite. Table 2 displays the interatomic distances of three shortest contacts. Upon the chemisorption at the O1-, O3-, and O4-site, respectively, the distances of all contacts are longer than 2.2 Å. Such contacts are therefore classified as weak (∼2.2 Å) or very weak (∼2.5 Å) hydrogen bonds[38] and cannot significantly influence the stability of the chemisorbed molecules. Moreover, the three shortest contacts between the molecule and the zeolite are very similar for all O-sites. The stability of the molecule chemisorbed at different O-sites therefore cannot be driven by the H···O contacts.

The analysis of bonding shows the following reasons for higher stability of alkoxy species at the O4-site: (i) the C−O bond at the O4-site is the shortest and therefore the most stabilizing, (ii) the hydrocarbon molecule adsorbed at the O4-site is relaxed into the most symmetrical shape.

4.3 Protonated Olefins. The static relaxation, that does not consider temperature effects, shows that chemisorbed species immobilized at specific sites of the zeolite surface (O4-site of gmelinite) can be more stable than physisorbed molecules (Figure 4). The difference between physi- and chemisorption energies for large molecules, however, is only several kJ/mol. At the same time for large molecules, both energy and geometry data indicate a strong repulsion between the molecule and the zeolite framework. Increased temperature enhances molecular species mobility. We therefore assume that with increasing temperature alkoxy species can easily desorb from the zeolite surface. To verify this assumption, we have performed ab initio molecular dynamical simulations at temperatures ranging between 400 and 700 K.[39] We have found that hydrocarbons can desorb either as neutral molecules or in the form of protonated species. The probability to desorb a neutral molecule, however, is much lower as it requires the back-transfer of the proton from

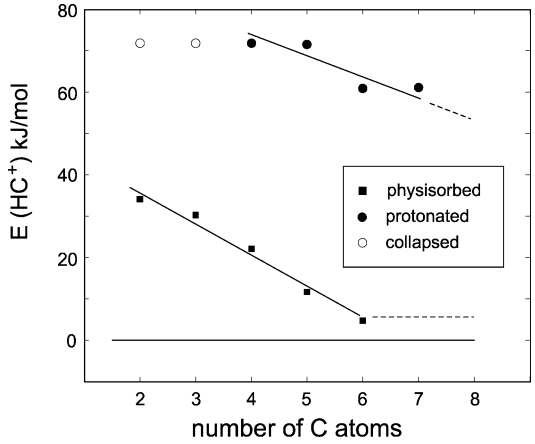

Figure 7. Energies of protonated olefins relative to the most stable chemisorbed species. Calculated energies of physisorption are displayed for comparison.

the molecule to the zeolite. Most simulations have lead to the desorption of a protonated molecule. Upon contact with the zeolite the protonated molecule might collapse to a neutral molecule leaving a protonated (acid) zeolite. Simulations have shown, however, that large molecules make no such contacts.[40] The positively charged particle is long-lived and accommodated approximately in the center of the channel.[40]

Long lifetimes of protonated olefins indicate the existence of local potential energy minima for the molecules placed in the channel. To compare the stabilities of protonated species in Figure 7 we display energies of carbocations formed upon protonation of several *n*-olefins. For ethene and propene no minima are localized. These particles deliver the proton back to the zeolite and convert to neutral molecules. The open circles in Figure 7 show energies prior to the collapse. Protonated butene and pentene both exhibit an energy ∼70 kJ/mol higher than that of the chemisorbed molecule. Protonation of larger molecules (hexene, heptene) produces more stable carbocations (∼60 kJ/mol). Larger stability originates in better capability of larger molecules to accommodate the positive charge. The calculated energies of protonated molecules thus demonstrate an increase of basicity with increasing length of the hydrocarbon molecule. Very long molecules are expected to be basic enough for allowing spontaneous transfer of the zeolite acid proton to the hydrocarbon molecule.

5 Conclusions

We have performed extensive periodic ab initio density-functional calculations of the zeolite framework containing adsorbed hydrocarbon molecules. Both physisorbed and chemisorbed molecules are considered. We compare the adsorption energy and bonding for series of linear molecules to bring together a complete picture of the adsorption of hydrocarbons in zeolites. Stabilities of protonated molecules, formed upon desorption of chemisorbed alkoxy species, are compared for several linear olefins.

For gmelinite, experimental adsorption energies are not available. The energies calculated for olefins show a linear increase with the length of the hydrocarbon and are in reasonable agreement with the estimates extrapolated from other zeolite structures. The calculated energies of paraffins, however, are ∼2.5 times smaller than the estimate of the experimental adsorption energy. Adsorbed saturated hydrocarbons are stabilized in zeolites through weak interactions, a major part of which is of dispersion van der Waals character. Because GGA functionals of density-functional theory does not account for dispersion dispersion interactions, the calculated adsorption energies are therefore much smaller than the experimental values.

Upon chemisorption of unsaturated hydrocarbons at the inner surface of the zeolite a covalent C−O bond between the molecule and the zeolite is formed, inducing a local deformation of both the molecule and the zeolite framework. The molecule is deformed in order to maximize the C-to-O contact and to minimize any other contact with the zeolite framework. Within the framework a change of Si−O and Al−O bond-lengths, and of Al−O−Si angles is observed. The C−O bond-length in the alkoxy species is more than 1.5% longer than corresponding bond in a simple C−OH hydroxide (∼1.485 Å). The shorter is the C−O bond, the more stable is the alkoxy species. Calculated energies show that the chemisorption at the O4-site provides a more stable alkoxy species than at the O1-, and O3-sites. With increasing length of the molecular chain the energy of chemisorption decreases due to the increase of the deformation energy and due to the increase of the repulsion between the molecule and the zeolite. Molecules longer than propene chemisorbed at O1- and O3-site are less stable than free physisorbed molecules. The decrease of the chemisorption energy for the O4-site, however, is less steep. Beginning with heptene an increase of the chemisorption energy is observed. Upon the extension of the chemisorbed hexene to heptene, a linear elongation of the free end of the molecule occurs. The repulsion between the free end of the molecule and the zeolite is small and the linear extension does not lead to any deformation. The energy of chemisorption therefore increases compared with the hexene molecule. A noticeable fact is that alkoxy species of any length adsorbed at the O4-site remain more stable than free physisorbed molecules. The O4-site thus represents the adsorption site for preferential chemisorption of unsaturated hydrocarbons. The gmelinite O4-site is distinguished by the smallest local deformation of bonding upon chemisorption. In addition, the shortest and most stabilizing O−C bond is formed and the molecule adsorbed at the O4-site retains more symmetric shape compared with the chemisorption at the other sites.

The relative stability of protonated hydrocarbons depends on the length of the molecule. Short molecules (ethene, propene) are found to be unstable and collapse to the neutral species. Protonated molecules longer than propene are stabilized and long-lived in the zeolite surroundings. Their energy is by ∼70 kJ/mol higher compared with the chemisorbed species (butene, pentene). For longer molecules further stabilization is observed as a result of better ability to delocalize the positive charge. Beyond some length, one can expect *n*-hydrocarbons to be spontaneously protonated in acid zeolites.

Acknowledgment. The work has been performed within the Groupement de Recherche Européen "Dynamique Moléculaire Quantique Appliquée à la Catalyse, founded by the Council National de la Recherche Scientifique (France), the Institut Français du Pétrole (IFP), TOTAL Recherche et Development, and the Universität Wien. Facilities at Computing Center of Vienna University (Schrödinger cluster) are kindly acknowledged.

References and Notes

(1) Corma, A. *Chem. Rev.* **1995**, *95*, 559.

(2) Kissin, Y. V. *Catal. Rev.* **2001**, *43*, 85.

(3) Haag, W. O.; Dessau, R. M. In *Proc. 8th Int. Congress on Catalysis*, Berlin, Vol. 2, Dechema, Frankfurt am Main, 1984; p 305.

(4) Kotrel, S.; Knözinger, H.; Gates, B. C. *Micropor. Mesopor. Mater.* **2000**, *35*−*36*, 11.
(5) Olah, G. A. *J. Org. Chem.* **2001**, *66*, 5943.
(6) Olah, G. A.; Prakash, G. K. S.; Sommer, J. *Superacids*; Wiley-Interscience: New York, 1995.
(7) Haw, J. F.; Richardson, B. R.; Oshiko, I. S.; Lazo, N. B.; Speed, J. A. *J. Am. Chem. Soc.* **1989**, *111*, 2052.
(8) Zardkoohi, M.; Haw, J. F.; Lunsford, J. N. *J. Am. Chem. Soc.* **1987**, *109*, 5278.
(9) Derouane, E. G.; He, H.; Hamid, S. B. D.-A.; Ivanova, I. I. *Catal. Lett.* **1999**, *58*, 1.
(10) Kazansky, V. B. *Catal. Today* **1999**, *51*, 419.
(11) Viruela, P.; Zicovich, C. M.; Corma, A. *J. Phys. Chem.* **1993**, *97*, 13 713.
(12) Boronat, M.; Viruela, P.; Corma, A. *J. Phys. Chem. A* **1998**, *102*, 982.
(13) Furtado, E. A.; Milas, I.; Lins, J. O. M. D. A.; Nascimento, M. A. C. *Phys. Stat. Sol.* (*a*) **2001**, *187*, 275.
(14) Rozanska, X.; van Santen, R. A.; Hutschka, F. Theoretical Study of Reactions Catalyzed by Acid Zeolite. In *Theoretical Aspects of Heterogeneous Catalysis*; Nascimento, M. A. C., Ed.; Kluwer: Amsterdam, 2001, p 1.
(15) Demuth, T.; Rozanska, X.; Benco, L.; Hafner, J.; vanSanten, R. A.; Toulhoat, H. *J. Catal.* **2003**, *214*, 68.
(16) Zygmunt, S. A.; Curtiss, L. A.; Zapol, P.; Iton, L. E. *J. Phys. Chem. B* **2000**, *104*, 1944.
(17) Ángyán, J.; Parsons, D. Ab Initio Simulations of Zeolite Reactivity. In *Theoretical Aspects of Heterogeneous Catalysis*; Nascimento, M. A. C., Ed.; Kluwer: Amsterdam, 2001, p 77.
(18) Boronat, M.; Zicovich-Wilson, C. M.; Viruela, P.; Corma, A. *J. Phys. Chem. B* **2001**, *105*, 11 169.
(19) Galli, E.; Passaglia, E.; Zanazzi, P. F. *N. Jb. Miner. Mh.* **1982**, *1982*, 1145.
(20) Baerlocher, C.; Meier, W. M.; Olson, D. H. *Atlas of Zeolite Framework Types*; Elsevier: Amsterdam, 2001.
(21) Benco, L.; Demuth, T.; Hafner, J.; Hutschka, F. *J. Chem. Phys.* **1999**, *111*, 7537.
(22) Jones, R. O.; Gunnarsson, O. *Rev. Mod. Phys.* **1989**, *61*, 689.
(23) Perdew, J. P.; Chevary, A.; Vosko, S. H.; Jackson, K. A.; Pedersen, M. R.; Singh, D. J.; Fiolhais, C. *Phys. Rev. B* **1992**, *46*, 6671.
(24) Perdew, J. P.; Wang, Y. *Phys. Rev. B* **1992**, 13 244.
(25) Vanderbilt, D. *Phys. Rev. B* **1990**, *41*, 7892.
(26) Kresse, G.; Hafner, J. *J. Phys. Cond. Matter* **1994**, *6*, 8245.
(27) Kresse, G.; Furthmüller, J. *Phys. Rev. B* **1996**, *54*, 11 169.
(28) Blöchl, P. E. *Phys. Rev. B* **1994**, *50*, 17 953.
(29) Kresse, G.; Joubert, D. *Phys. Rev. B* **1999**, *59*, 1758.
(30) Benco, L.; Demuth, T.; Hafner, J.; Hutschka, F.; Toulhoat, H. *J. Chem. Phys.* **2001**, *114*, 6327.
(31) Sun, M.; S.; Talu, O.; Shah, D. B. *J. Phys. Chem.* **1996**, *100*, 17 276.
(32) Denayer, J. F.; Baron, G. V.; Martens, J. A.; Jacobs, P. A. *J. Phys. Chem. B.* **1998**, *102*, 3077.
(33) Eder, F.; Lercher, J. A. *J. Phys. Chem. B* **1997**, *101*, 1273.
(34) Breck, D. W. *Zeolite Molecular Sieves*; Wiley: New York, 1974.
(35) Dixit, L.; Prasada Rao, T. S. R. *J. Chem. Inf. Comput. Sci.* **1999**, *39*, 218.
(36) Eder, F.; Lercher, J. A. *Zeolites*, **1997**, *18*, 75.
(37) Demuth, T.; Benco, L.; Hafner, J.; Toulhoat, H.; Hutschka, F. *J. Chem. Phys.* **2001**, *114*, 3703.
(38) Benco, L.; Smrcok, L. *Eur. J. Mineral.* **1998**, *10*, 483.
(39) Benco, L.; Demuth, T.; Hafner, J.; Hutschka, F.; Toulhoat, H., unpublished results.
(40) Benco, L.; Demuth, T.; Hafner, J.; Hutschka, F.; Toulhoat, H. *J. Catal.* **2002**, *205*, 147.